Bifunctional Separator with a Light-Weight Carbon-Coating for Dynamically and Statically Stable Lithium-Sulfur Batteries

*Sheng-Heng Chung and Arumugam Manthiram**

Sulfur is appealing as a high-capacity cathode for rechargeable lithium batteries as it offers a high theoretical capacity of 1672 mA h g^{-1} and is abundant. However, the commercialization of Li-S batteries is hampered by fast capacity fade during both dynamic cell cycling and static cell resting. The poor electrochemical stability is due to polysulfide diffusion, leading to a short cycle life and severe self-discharge. Here, we present the design of a bifunctional separator with a light-weight carbon-coating that integrates the two necessary components already inside the cell: the conductive carbon and the separator. With no extra additives, this bifunctional carbon-coated separator allows the use of pure sulfur cathodes involving no complex composite synthesis process, provides a high initial discharge capacity of 1389 mA h g^{-1} with excellent dynamic stability, and facilitates a high reversible capacity of 828 mA h g^{-1} after 200 cycles. In addition, the static stability is evidenced by low self-discharge and excellent capacity retention after a 3 month rest period.

1. Introduction

Rechargeable batteries with a high capacity, acceptable cycle life, and low self-discharge are needed for meeting the ever-increasing requirements of energy storage applications, from personal electronic devices to large-scale sustainable energy systems. Safe, cost-effective, and environmentally benign materials and manufacturing processes must also be pursued to meet the needs of manufacturing and global sustainability. Sulfur is abundant and environmentally benign and it offers higher theoretical capacity (1672 mA h g^{-1}) at a safer operating voltage (≈2.1 V) compared to the conventional insertion-compound cathodes. Thus, the lithium-sulfur (Li-S) battery fulfills all of the above criteria and is considered to be a promising high-capacity system.[1] However, the commercialization of Li-S cells is hampered by several technical challenges: (i) low electrochemical utilization, (ii) short cycle life, and (iii) severe self-discharge.[2] Effective utilization of the high capacity is difficult with a pure sulfur cathode due to the insulating nature of both sulfur and its discharge end product (Li_2S_2/Li_2S).[1b,2a,c] Moreover, during the discharge/charge processes, sulfur converts to highly soluble polysulfides (Li_2S_x, $4 < x \leq 8$). The polysulfides easily dissolve into the liquid electrolyte, diffuse through the separator, and shuttle between the anode and cathode. The loss of the active material and the shuttling species lead to "dynamic" capacity fade during cycling, resulting in low Coulombic efficiency and short cycle life.[2b–d] Moreover, during cell resting, sulfur gradually reacts with the lithium ions in the electrolyte, transforms to polysulfides, and dissolves into the electrolyte, resulting in severe self-discharge. The polysulfide diffusion that occurs during cell storage results in a "static" decrease in cell capacity.[2b,d]

To address these scientific issues, current Li-S technology has focused on improving the electrical conductivity of the "composite" sulfur cathode and localizing the active material within the cathode region of the cell. These promising approaches include sulfur-porous carbon composites,[3] sulfur-conductive polymer composites,[4] binder/electrolyte additives,[5] cell configuration modifications,[6] and biomimetic archetictures.[7] These approaches function as various kinds of quick cures and have shown i) higher discharge capacity through a decrease in cathode resistance with the addition of conductive species,[3–7] ii) improved cyclability through the confinement of the migrating polysulfides by porous agents and chemical characteristics,[3–5,7a] or iii) suppressed polysulfide diffusion by localizing the electrolyte containing dissolved polysulfides within the cathode regions.[6,7b,c] However, quick cures often cause some side effects while they address the major issues. For example, the nanocomposite cathodes often involve complex/unpractical multistep processes and modified cell configurations usually require a unique "free-standing component." In addition, the reduced sulfur content in the composite cathodes and the added weight of the applied free-standing component in cell modifications may lead to new concerns of a decrease in overall energy density, which may cancel off the gains in cell performance, e.g., cycle life.

Here, we present a bifunctional separator with a light-weight carbon-coating (C-coating) for use with pure sulfur cathodes, which is a facile and practical solution. The carbon-coated (C-coated) separator integrates two necessary, cost-effective, and commonly used components that are already present inside the cell: the conductive carbon black (Super P carbon) and the

S.-H. Chung, Prof. A. Manthiram
Electrochemical Energy Laboratory and Materials Science and Engineering Program
The University of Texas at Austin
Austin, TX 78712, USA
+1–512–471–1791
+1–512–471–7681
E-mail: manth@austin.utexas.edu

DOI: 10.1002/adfm.201400845

polymeric separator (Celgard separator).[8] The architecture of the C-coated separator consists of a layer of Super P thin film coated on one side of the Celgard separator. The bifunctional C-coating functions as a conductive upper current collector and a polysulfide-diffusion barrier region while the Celgard separator serves as the electrically insulating membrane.

As a result, the C-coated separator allows the pure sulfur cathode to reach a high initial discharge capacity approaching 1400 mA h g^{-1} and a reversible capacity of 828 mA h g^{-1} after 200 cycles at a C/5 rate. The C rates are based on the mass and theoretical capacity of sulfur (1C = 1672 mA h g^{-1}). The C-coated separator leads to excellent rate capability (up to 2C rate) and a high Columbic efficiency of ≈98%. The self-discharge rate is as low as 0.19% per day after resting for three months. Moreover, the light-weight C-coating layer is only 0.2 mg cm^{-2} (the weight of the Celgard separator is 1.0 mg cm^{-2}), which overcomes the drawbacks of the low sulfur content issue of the composite cathodes and the added significant weight of the free-standing components employed in cell modifications. The commercialization feasibility of Li-S cells greatly depends on overcoming the severe cell stability challenges with practical solutions that can be easily translated into industrial processes. Here, we demonstrate such a solution by introducing a C-coated separator, which greatly enhances the dynamic and static performance of Li-S cells, while utilizing low-cost materials and simple processing techniques.

2. Results and Discussion

2.1. Configuration and Characterization of the C-coated Separator

Figure 1a presents the C-coated separator that consists of a light-weight conductive C-coating on one side of a polypropylene separator. The C-coated side of the separator faces the pure

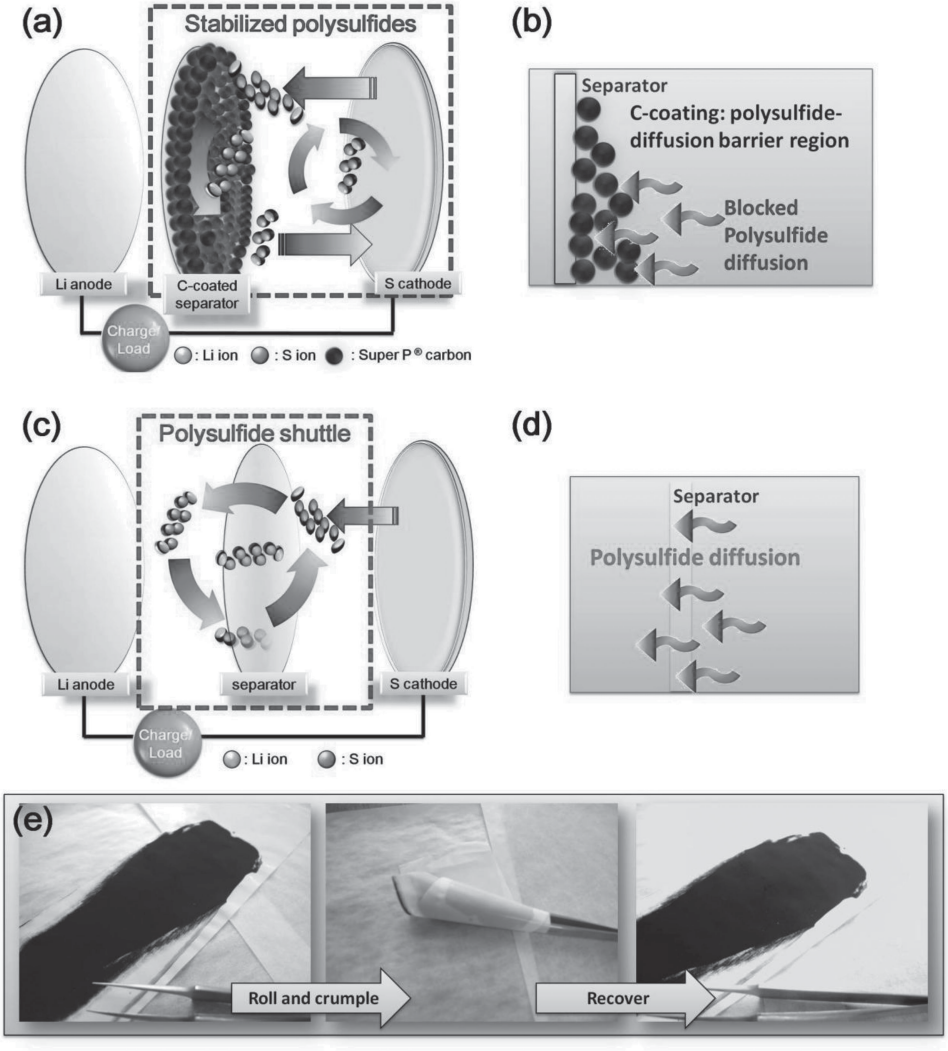

Figure 1. Schematic cell configuration modification of Li-S cells. a) Schematic configuration of a Li-S cell with the C-coated separator and b) the polysulfide-diffusion barrier region. c) Schematic configuration of a Li-S cell with the Celgard separator and d) the typical severe polysulfide diffusion. e) Demonstration of the flexibility and mechanical strength of the C-coated separator.

sulfur cathode and acts as a barrier region (with the thickness of ≈20 µm). In Figure 1b, the C-coating barriers aim at impeding the free migration of the polysulfides and preventing them from smoothly diffusing through the Celgard separator.[6e,f] Moreover, this conductive C-coating offers additional electron pathways for the insulating sulfur cathode and functions as the "upper" current collector to accelerate fast electron transport.[6d,e] During long-term cycling, this upper current collector easily transports electrons into the intercepted active material to reactivate them. Therefore, high sulfur utilization and effective active material reutilization are accomplished.[6d,e] On the other side, the insulating Celgard remains highly electronically resistive. For a comparison, Figure 1c shows the schematic cell configuration of the conventional Li-S cell, suffering from the issues described above, especially the severe polysulfide diffusion issue (Figure 1d).

It is worth emphasizing that the weight of the C-coating is only 0.2 mg cm^{-2}, much lighter than the weight of the Celgard separator (1.0 mg cm^{-2}). Therefore, even as we include the weight of the C-coating, the cell with the C-coated separator allows a high sulfur content of above 55 wt% in the whole cathode region, higher than that in most high-performance Li-S cells.[9] Moreover, the C-coated separator has good flexibility and mechanical strength, as shown in Figure 1e, allowing it to retain its normal function during cell cycling.

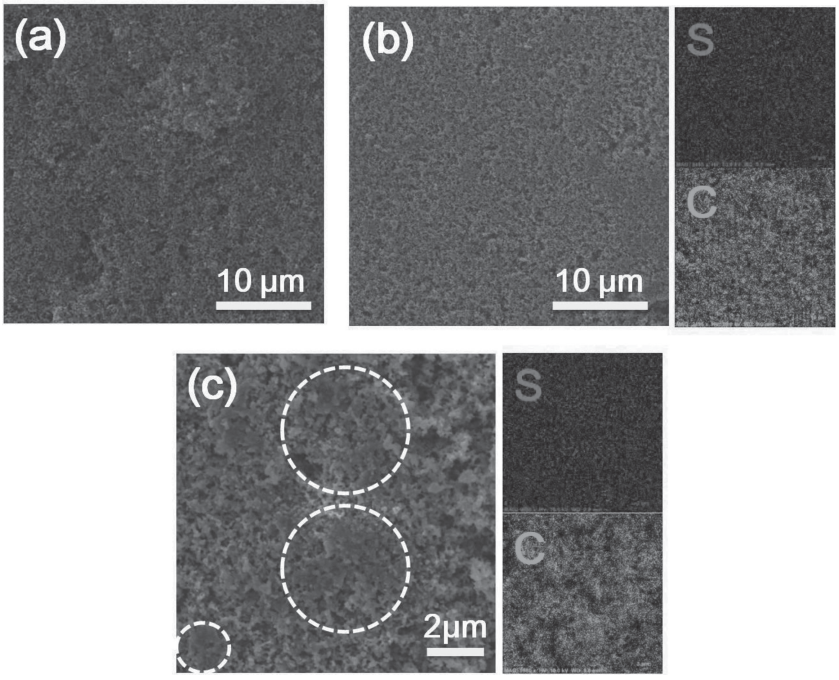

Figure 2. Morphology and elemental analyses of the C-coated separator. a) SEM observation of the C-coated separator before cycling. SEM observation and elemental mapping of the C-coated separator after cycling: b) wide-range morphological observation and c) local microstructural observation.

2.2. Morphological and Elemental Mapping Analyses of the Cycled C-coated Separator

To demonstrate the efficacy of the C-coated separator, the morphological changes before and after cycling were analyzed by scanning electron microscopy (SEM) and elemental mapping was performed with energy-dispersive X-ray spectroscopy (EDX), as summarized in **Figure 2**. Figure 2a shows that the surface of the fresh C-coated separator consists of a layer of porous nanoparticle clusters uniformly attached to the polypropylene separator. The porous structure of the C-coating allows the liquid electrolyte to freely penetrate through the coating layer, ensuring that the electrochemical reaction proceeds in the cathode.[6d,e] However, the C-coating can i) work as barriers for suppressing the free diffusion of polysulfides and ii) function as absorption agent for localizing the electrolyte containing the dissolved polysulfides within the cathode region of the cell.[6e,f,i],[10] To support this statement, low-magnification SEM and elemental mapping of the C-coated separator after 200 cycles are shown in Figure 2b. The overlays of the sulfur EDX signal (marked as red) and the carbon EDX signal (marked as green) on the SEM image show that the sulfur-containing species are uniformly distributed on the carbon matrix. This demonstrates that the C-coating effectively intercepts the dissolved polysulfides within its barrier region. As a further evidence, in the high magnification SEM image (Figure 2c), the obstructed active material (marked in white) is observed on the surface of the C-coating.

The fact that there are no large agglomerates on the C-coating in both Figure 2b and 2c suggests that the obstructed active material is continuously reutilized and that there is no formation of large insulating precipitates during long-term cycling. Both of these are vital to solving the severe capacity fade in Li-S cells.[11] These enhancements may result from i) the high conductivity of the Super P network, which supplies electrons to reactivate the trapped species[6d] and ii) the nanoscale Super P clusters of the C-coating that limits the formation of large precipitates.[3a] As evidenced, the elemental sulfur signals (Figure 2b and 2c) show no obvious dense spots and the elemental carbon signals are still strong.

The cross-sectional SEM and elemental mapping conducted on cells after 200 cycles demonstrate how the C-coated separator suppresses the severe polysulfide diffusion (Figure 1b and 1d). **Figure 3**a shows a cross-section of the cell, with (from left to right) the Super P C-coating (≈20 µm), pure sulfur cathode (≈40 µm), and Al current collector. The Celgard separator was carefully removed to avoid the electron beam charging. Evidence of the polysulfide interception mechanism can be found in the results of the elemental sulfur mapping (Figure 3b), which shows obvious sulfur concentration changes: i) lack of sulfur at the interface of the C-coating and sulfur cathode[7b,c] and ii) decrease in sulfur concentration within the C-coating.[6e,7b,c] The sulfur concentration gap demonstrates that most of the polysulfides were obstructed on the surface of the C-coating.

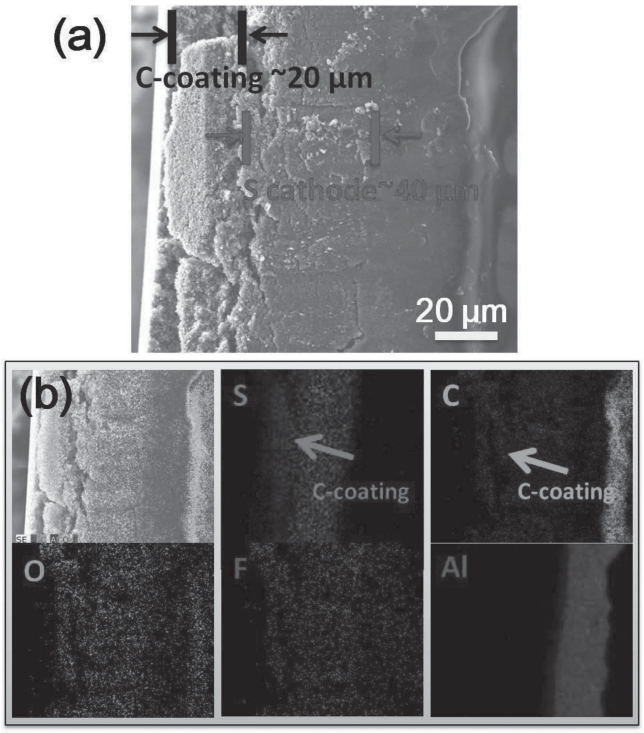

Figure 3. Microstructural analysis of a cell with the C-coated separator. a) Cross-sectional SEM observation and b) elemental mapping of the C-coating and cathode configuration.

Then, in the C-coating, there is a sulfur concentration gradient, with stronger sulfur signals pointing towards the cathode and weaker signals towards the separator. This further demonstrates that the nanoparticle cluster network serves as the barrier region to obstruct and immobilize the migrating polysulfides before they are able to penetrate through the C-coating. This conclusion is well supported by the SEM inspection on the Celgard side of the cycled C-coating in Figure S1a. On this side, the C-coating retains its porous structure and no obvious trapped active material can be found. The corresponding elemental mapping results in Figure S1b also exhibit weak sulfur signals and strong carbon signals, reconfirming that the intercepted active materials cannot reach the Celgard separator. In addition, the elemental carbon signals in Figure 3b are also discernible, suggesting that the intercepted active materials do not grow into insulating agglomerates and block the porous electrolyte channels but rather are continuously reactivated and thus contribute to the capacity.[6d,7b,c]

2.3. Electrochemical Analyses of the Pure Sulfur Cathode Utilizing the C-coated Separator

Based on the visual inspection of the morphological changes of the C-coating presented in Figure 2 and 3, it is reasonable to expect that the conductive C-coating can facilitate smooth electron transport between the insulating active material and the electrical conductor. This may facilitate i) a low resistance and ii) excellent reutilization of the trapped active material. To identify these enhancements, electrochemical impedance analysis was used to compare the impedance/resistance of the cell with the C-coated separator to that of a cell with a standard Celgard separator. The electrochemical impedance spectroscopy (EIS) data of the cells with different separators indicate that the charge transfer resistance (R_{ct}, in the high-frequency region) decreases by over 75% after replacing the Celgard separator by the C-coated separator, as shown in Figure S2. This demonstrates a significant decrease in the cathode resistance. After cycling, the impedance semicircles of the C-coated separator are much smaller than those of the Celgard separator. This is because the C-coating functions as the conductive network to reactivate the intercepted active material, so it limits the formation of insulating active material agglomerates. The EIS data thus demonstrate low cathode resistance and reutilization the trapped active material.

It is well known in the literature that a low cathode resistance and successive reutilization of the active material are vital to, respectively, increasing the active material utilization and extending the cycle life.[2b,3a,6d] These improvements are identified by a comparison of the discharge/charge voltage profiles during the initial 20 cycles at a C/5 rate of cells with different separators, as presented in **Figure 4**a and 4b. Figure 4a shows the discharge/charge curves of the cell utilizing the C-coated separator. During discharge, the two separate plateaus indicate the occurrence of the two complete reduction reactions.[12] The upper discharge plateau at ≈2.35 V corresponds to the first reduction from elemental sulfur (S_8) to long-chain polysulfides (Li_2S_x, $4 < x \leq 8$). The corresponding discharge capacity (Q_H) is 416 mA h g^{-1} approaching 99% of the theoretical value (419 mA h g^{-1}), implying limited polysulfide diffusion.[12a] The lower discharge plateau at ≈2.05 V represents the second reduction from long-chain polysulfides to short-chain Li_2S_2/Li_2S.[12a] As seen in Figure 4a and Figure 4b, the C-coating increases the initial discharge capacity from 1051 to 1389 mA h g^{-1}, demonstrating improved sulfur utilization (from 63% to 83%), consistent with the EIS analysis. In the subsequent cycles, the upper discharge plateaus are well-retained, which provides evidence that the C-coating successfully intercepts the escaping polysulfides and limits the loss of the active material. Moreover, the overlapped discharge curves demonstrate that the C-coating continuously reactivates the trapped active material, leading to stable cell cycling. During charge, the two continuous plateaus at ~2.25 and ~2.4 V are attributed to the reversible oxidation reactions of Li_2S_2/Li_2S to Li_2S_8/S_8. As the voltage approaches 2.8 V, the vertical rise in voltage indicates a complete charge reaction.[2b,11,13] Similarly stable cycling performance is observed in cells employing the C-coated separator at various cycling rates (Figure S3, see ESI).

The suppressed polysulfide diffusion is confirmed by an investigation of the upper discharge voltage plateaus and their corresponding capacities. This upper plateau region corresponds to the formation of highly soluble polysulfides.[2c],d In Figure 4a, the upper discharge voltage plateaus of the cells with the C-coated separator remain complete and show almost no decrease in capacity. For the sake of comparison, Figure 4b shows that the upper discharge plateaus of the cells with the Celgard separator exhibit the typical plateau shrinkage along with severe capacity fade. The upper plateau capacities of cells with different separators are summarized in Figure 4c. The

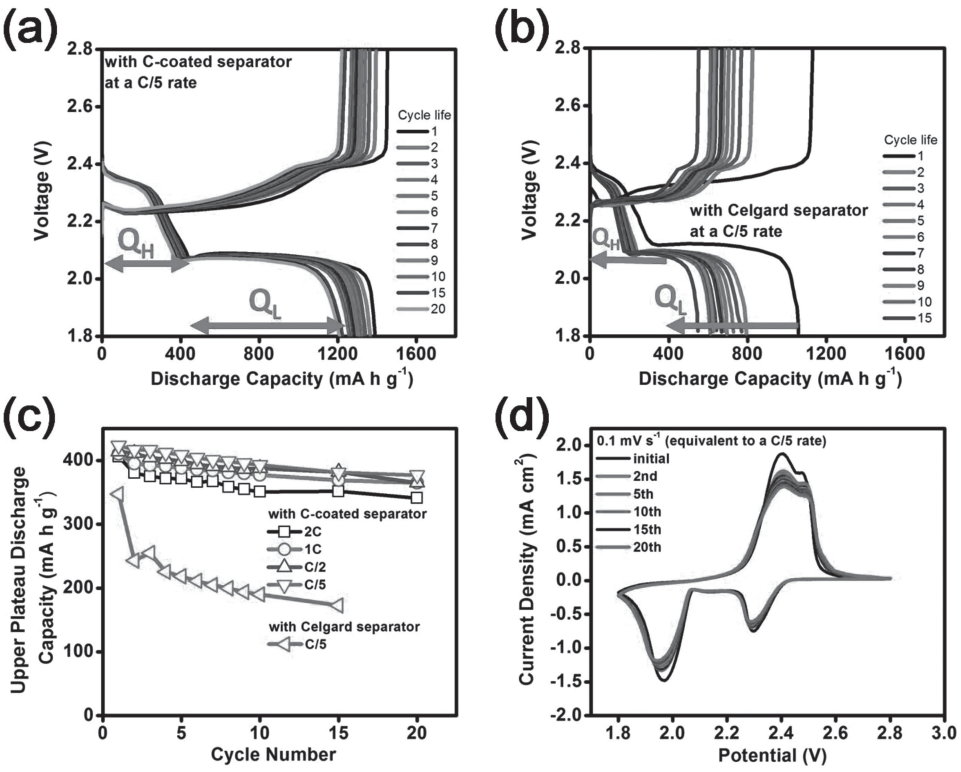

Figure 4. Electrochemical measurements of Li-S cells. Discharge/charge curves of cells: a) C-coated separator, b) Celgard separator, and c) upper plateau discharge capacities of cells employing different separators at various cycling rates. d) Cyclic voltammograms of the cell with the C-coated separator.

upper plateau capacities of the cells with the C-coated separator remain highly reversible at various cycling rates. However, the upper plateau capacity of the Celgard separator-only cell decreases to 45% of its original value after 10 cycles at a C/5 rate. This enhancement demonstrates that the C-coating effectively suppresses the diffusion of polysulfides and thus eliminates the severe loss of active material/capacity during cell cycling.

The enhanced cycle stability is further illustrated by the overlapping curves of the cyclic voltammograms (CVs), as shown in Figure 4d. The two cathodic peaks and the two overlapped anodic peaks are consistent with the discharge/charge curves. Notably, there are no apparent current or potential changes in these CV peaks with repeated scans, attesting to superior cell reversibility and stability.

2.4. Dynamically and Statically Electrochemical Stability of the Pure Sulfur Cathode Utilizing the C-coated Separator

Figure 5a demonstrates that the C-coated separator leads to significant enhancements in the dynamic electrochemical stability of the pure sulfur cathode, as evidenced by the high discharge capacity and stable cyclability. The pure sulfur cathodes achieve initial discharge capacities of 1389, 1289, 1220, and 1045 mA h g^{-1} at, respectively, C/5, C/2, 1C, and 2C rates. After 50 cycles, the reversible capacities approach 1112, 1074, 1021, and 920 mA h g^{-1} which corresponds to capacity retentions of, respectively, 80, 83, 84, and 88%. The stable cyclability allows the cells to remain highly reversible over a wide range of cycling rates, from C/5 to 2C. As a comparison, the pure sulfur cathode with a Celgard separator has an initial capacity of 1051 mA h g^{-1} (marked as black) at a C/5 rate, which decreases to 785 mA h g^{-1} after the second cycle. Moreover, the discharge capacity after 50 cycles is only 500 mA h g^{-1}, indicating that long-term cycling is not feasible with this type of cell.

On the other hand, the high electrochemical reversibility of the C-coated separator ensures the cell to accomplish long-term cyclability over 200 cycles, with the capacity fading as low as 0.20% per cycle, as shown in the Figure 5b. The long-term cyclability may result from the successive interception, reactivation, and reutilization of polysulfides in the nano-sized conductive C-coating, concomitantly stabilizing the electrochemical reactions and the active material within the cathode region during long cycle life. The reversible capacity of the cells (with the calculated capacity fading in parentheses) cycling at C/5, C/2, 1C, and 2C rates after 200 cycle are, respectively, 828 (0.20%), 810 (0.19%), 771 (0.18%), and 701 mA h g^{-1} (0.16%). The average Coulombic efficiencies at various cycling rates are above 98.2%. The addition of a small amount of $LiNO_3$ co-salt in the electrolyte can protect the lithium anode by forming a passivation layer on its surface, and effectively enhance the Coulombic efficiency to above 90%.[14] The application of the C-coated separator further improves the efficiency from 92% to 98%. In addition, no fast capacity fade can be found in the cells with the C-coated separator during long-term cycling, indicating that

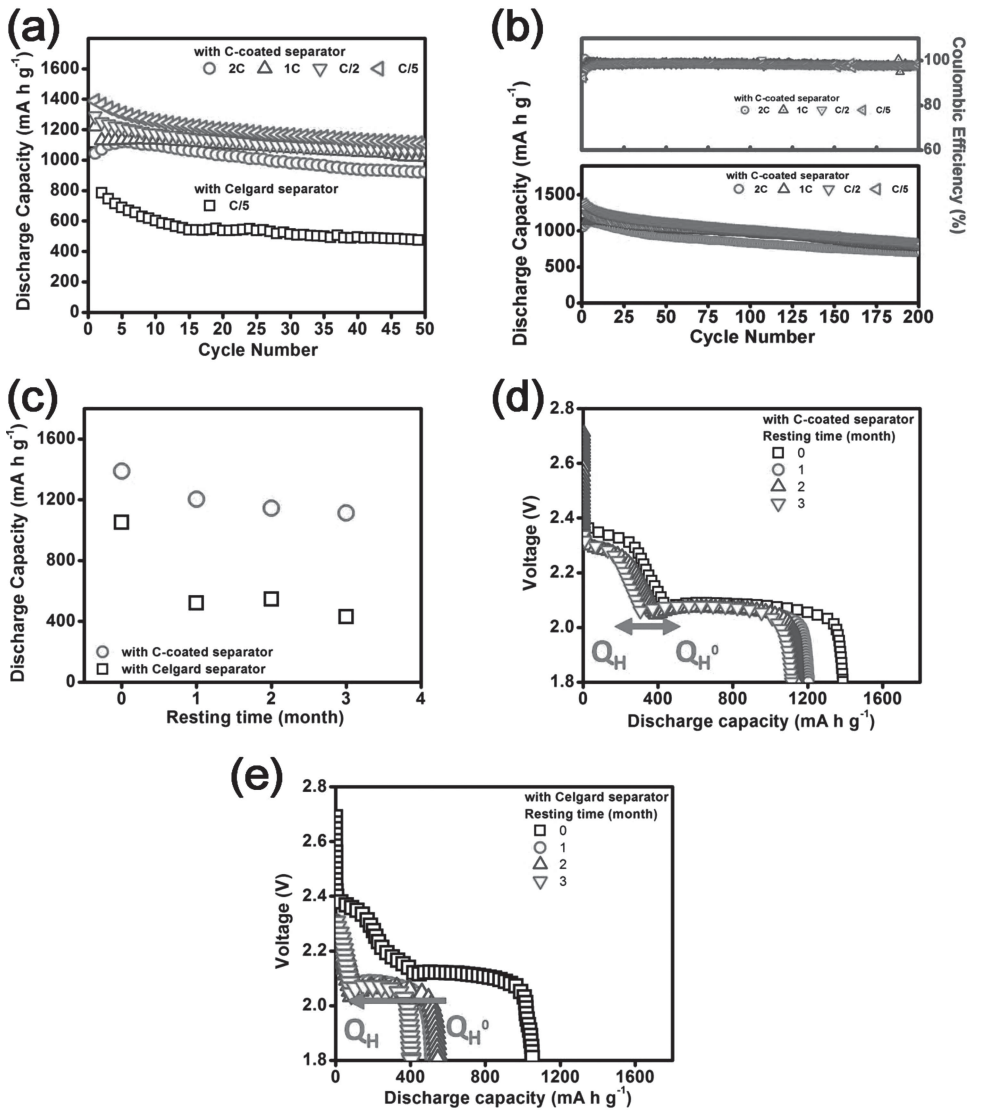

Figure 5. Cell performance of Li-S cells. Dynamic electrochemical stability: a) cycle stability and b) long-term cycle life of the cells with different separators at various cycling rates. Static electrochemical stability: c) self-discharge behavior of the cells with different separators with various storage times. Initial discharge curves after different storage times employed with cells consisting of d) C-coated separator and e) the Celgard separator.

the C-coating remains intact with good mechanical strength and normal function during cycling.[6g] Such good mechanical integrity of the C-coating may result from the physical adsorption between the carbon nanoparticles and the porous Celgard separator, avoiding the peeling-off of the C-coating from the Celgard separator.[6h] The superior cycling stability suggests that the C-coated separator provides a more stable electrochemical environment for the pure sulfur cathode than that found with the conventional cells.

Li-S cells also suffer from self-discharge that occurs due to polysulfide diffusion during cell rest.[2c,d],[15] The success of the C-coated separator in mitigating the cell instability during cycling has also been investigated for reducing this self-discharge. In Figure 5c, the conventional cells with the Celgard separator (marked in black) could not limit the static polysulfide diffusion and, therefore, show the typical self-discharge behavior during cell rest. After one month of resting, the initial discharge capacity decreases from 1051 to 520 mA h g^{-1}, a loss of more than half of the original capacity. After three months, the severe self-discharge causes static capacity fading as high as 0.60% per day. On the other hand, the same pure sulfur cathode in a cell employing the C-coated separator (marked in red) manifests superior static capacity retention. In the first month, the cell retains 86% of its original capacity. In the subsequent two months, the capacity fading is almost negligible and the cell maintains 81% of its original capacity. The static capacity fading is around 0.19% per day over a 3-month period, implying a good suppression of the self-discharge behavior. The low self-discharge is attributed to the C-coated separator, which acts as a polysulfide fishnet and confines the active material within the cathode region of the cell during cell rest.

Detailed analysis of the self discharge behavior is summarized in the comparison of Figure 5d and 5e. Figure 5d shows the discharge curves of cells with the C-coated separator

after various rest times. After resting for a period of one month, the cell capacity shows a slight decrease from 1389 to 1204 mA h g^{-1}, then becomes mostly stable after that point. The complete shape of the upper voltage plateaus and the overlapping of the discharge curves indicate that the active material is well retained within the cathode region of the cell. In contrast, cells with the Celgard separator exhibit obvious capacity fading and a severe reduction of the upper discharge plateau after resting for one month, as seen in Figure 5e. The disappearance and shrinkage of the discharge plateaus result from the dissolution of sulfur and the subsequent formation of inactive precipitates during long-term storage, corresponding to severe cathode degradation and unstoppable static capacity fading.[15] The active material dissolution leads to the formation of pits on the cathode surface and the formation of insulating precipitates (Figure S4, see ESI). These features are not easily identified on the cathode with a C-coated separator (Figure S5, see ESI). Even after resting for 3 months, the C-coated separator cells exhibit good cycling stability (Figure S6, see ESI).

Based on these electrochemical and microstructural results, it is possible to conclude that the severe self-discharge has been appreciably attenuated in cells applying the C-coated separator. To support this statement, it is instructive to compare the self-discharge constants of both separators by a mathematical model (Figure S7, see ESI):[2d,6b]

$$\ln\left(\frac{QH}{QH^{\circ}}\right) = -K_s \times T_R$$

The self-discharge constant (K_s) can be determined by comparing the upper plateau discharge capacity (Q_H) and the initial upper plateau discharge capacity ($Q_H{}^0$) with the resting time, (T_R). The C-coated separator shows the low K_S of 0.05 per month, which is the lowest K_S compared to other self-discharge data on the Li-S cells.[2d,6b] In contrast, the K_S of the Celgard separator is as high as 0.44 per month. The low K_S demonstrates that the C-coating functions as a protective layer for the pure sulfur cathode, keeping the active material from dissolving into the electrolyte during long-term storage. Therefore, this separator configuration modification eliminates the severe loss of active material and the irreversible capacity fading problem of pure sulfur electrodes during cell rest.

3. Conclusion

In conclusion, the C-coated separator, that combines and rearranges two necessary components in Li-S cells, the Super P conductive carbon and the Celgard separator, is a facile, lightweight, and cost-effective separator configuration modification for improving Li-S batteries. After applying the C-coated separator, cells with the pure sulfur cathode accomplish both dynamic and static cycle stability. The enhanced cycling performance was demonstrated with higher sulfur content and a simpler fabrication method than those of many composite sulfur cathodes. In addition, the electrochemical analyses of the upper discharge plateau and their corresponding capacities that are effective for determining the dynamic and static stability of the Li-S battery solidly confirm the high performance of the C-coated separator.

4. Experimental Section

Carbon-Coated Separator Preparation: The C-coated separator was fabricated by surface coating commercial conductive carbon black (Super P, TIMCAL) on one side of a commercial polypropylene separator (CELGARD). The carbon slurry was prepared by mixing Super P carbon with isopropyl alcohol (IPA) overnight. The carbon slurry was coated onto the Celgard separator by the tape casting method and then dried for 24 h at 50 °C in an air oven. The application of the tape casting method, which is commonly used in cathode preparation, for the C-coated separator fabrication makes the processing facile and easily adaptable for large-scale applications. The C-coated separator was then cut into circular disks and inserted into coin cells with the carbon side facing the cathode. The fabrication process may be further simplified by drying the C-coated separator in air for 30 min (Figure S8, see ESI).

Pure Sulfur Cathode Preparation: The active material slurry was prepared by mixing 60 wt.% precipitated sulfur, 20 wt% Super P, and 20 wt% polyvinylidene fluoride (PVDF, Kureha) in N-methyl-2-pyrolidone (NMP) for 2 days. The active material slurry was tape-casted onto an Al foil current collector and dried for 24 h at 50 °C in an air oven, followed by roll-pressing and cutting into circular disks. In this work, the pure sulfur cathode refers to the basic cathode material containing only the necessary components: sulfur, conductive carbon additive, and binder.[8] The sulfur loading in the regular cathode disk is 1.1–1.3 mg cm^{-2}.

Cell Assembly: The CR2032-type coin cells were assembled with the pure sulfur cathode, C-coated separator, and lithium anode (Aldrich) in an argon-filled glove box. The separators and cathodes were dried in a vacuum oven for one hour at 50 °C prior to cell assembly. The electrolyte contained 1.85 M $LiCF_3SO_3$ salt (Acros Organics) and 0.1 M $LiNO_3$ co-salt (Acros Organics) in a 1:1 volume ratio of 1, 2-dimethoxyethane (DME; Acros Organics) and 1,3-dioxolane (DOL; Acros Organics). The assembled Li-S cells were allowed to rest for 30 min at 25 °C before electrochemical cycling. The cycled C-coated separators, cycled sulfur cathodes, and fresh sulfur cathodes after resting were retrieved inside an argon-filled glove box and stored in an argon-filled sealed vessel prior to analysis.

Characterization: The morphological changes of the C-coated separator before and after cycling were inspected with a scanning electron microscope (SEM) (JEOL JSM 5610) and a field emission scanning electron microscope (FE-SEM) (FEI Quanta 650). Both SEMs are equipped with energy dispersive X-ray spectrometers (EDX) for collecting elemental signals and mapping.

Electrochemical Measurements: The electrochemical impedance spectroscopy (EIS) data were obtained with an impedance analyzer (SI 1260 and SI 1287, Solartron) from 1 MHz to 100 mHz with an AC voltage amplitude of 5 mV. The cyclic voltammograms (CV) were recorded with a potentiostat (VoltaLab PGZ 402, Radiometer Analytical) with a voltage window of 1.8–2.8 V at a scan rate of 0.1 mV s^{-1}. The discharge/charge voltage profiles and cyclability data were collected with a programmable battery cycler (Arbin Instruments) with a voltage window of 1.8–2.8 V at various cycling rates from C/5 to 2C. The cutoff potential of 1.8 V is to avoid an irreversible reduction at ≈1.6 V that results from the $LiNO_3$ co-salt.[14] The self-discharge behaviors of the cells were investigated by measuring the initial discharge capacity of the cells after different rest times.

Supporting Information

Supporting Information is available from the Wiley Online Library or from the author.

Acknowledgements

This work was supported by the US Department of Energy, Office of Basic Energy Sciences, Division of Materials Sciences and Engineering under award number DE-SC0005397.

Received: March 15, 2014
Revised: April 14, 2014
Published online: June 24, 2014

[1] a) P. G. Bruce, S. A. Freunberger, L. J. Hardwick, J. M. Tarascon, *Nat. Mater.* **2012**, *11*, 19; b) X. L. Ji, L. F. Nazar, *J. Mater. Chem.* **2010**, *20*, 9821.

[2] a) A. Manthiram, Y. Fu, Y.-S. Su, *Acc. Chem. Res.* **2013**, *46*, 1125; b) S. S. Zhang, *J. Power Sources* **2013**, *231*, 153; c) J. R. Akridge, Y. V. Mikhaylik, N. White, *Solid State Ionics* **2004**, *175*, 243; d) Y. V. Mikhaylik, J. R. Akridge, *J. Electrochem. Soc.* **2004**, *51*, A1969.

[3] a) X. L. Ji, K. T. Lee, L. F. Nazar, *Nat. Mater.* **2009**, *8*, 500; b) C. Liang, N. J. Dudney, J. Y. Howe, *Chem. Mater.* **2009**, *21*, 4724; c) N. Jayaprakash, J. Shen, S. S. Moganty, A. Corona, L. A. Archer, *Angew. Chem. Int. Ed.* **2011**, *50*, 5904; d) J. Schuster, G. He, B. Mandlmeier, T. Yim, K. T. Lee, T. Bein, L. F. Nazar, *Angew. Chem. Int. Ed.* **2012**, *51*, 3591; e) J. Liu, T. Yang, D.-W Wang, G. Q. Lu, D. Zhao, S. Z. Qiao, *Nat. Commun.* **2013**, *4*, 2798; f) J. Song, T. Xu, M. L. Gordin, P. Zhu, D. Lv, Y.-B. Jiang , Y. Chen, Y. Duan, D. Wang, *Adv. Funct. Mater.* **2014**, *24*, 1242; g) L. Wang, Y. Zhao, M. L. Thomas, H. R. Byon, *Adv. Funct. Mater.* DOI: 10.1002/adfm.201303080; h) Z. Zhang, Z. Li, F. Hao, X. Wang, Q. Li, Y. Qi, R. Fan, L. Yin, *Adv. Funct. Mater.* DOI: 10.1002/adfm.201303080; i) H.-J. Peng, J.-Q. Huang, M.-Q. Zhao, Q. Zhang, X.-B. Cheng, X.-Y. Liu, W.-Z. Qian, F. Wei, *Adv. Funct. Mater.* DOI: 10.1002/adfm.201303296.

[4] a) J. Wang, J. Yang, J. Xie, N. Xu, *Adv. Mater.* **2002**, *14*, 963; b) L. Xiao, Y. Cao, J. Xiao, B. Schwenzer, M. H. Engelhard, L. V. Saraf, Z. Nie, G. J. Exarhos, J. Liu, *Adv. Mater.* **2012**, *24*, 1176; c) Y. Z. Fu, A. Manthiram, *J. Phys. Chem. C* **2012**, *116*, 8910.

[5] a) J. Wang, Z. Yao, C. W. Monroe, J. Yang, Y. Nuli, *Adv. Funct. Mater.* **2013**, *23*, 1194; b) W. Weng, V. G. Pol, K. Amine, *Adv. Mater.* **2013**, *25*, 1608; c) Z. Lin, Z. Liu, W. Fu, N. J. Dudney, C. Liangi, *Adv. Funct. Mater.* **2013**, *23*, 1064; d) J. Kim, D.-J. Lee, H.-G. Jung, Y.-K. Sun, J. Hassoun, B. Scrosati, *Adv. Funct. Mater.* **2013**, *23*, 1076.

[6] a) R. Elazari, G. Salitra, A. Garsuch, A. Panchenko, D. Aurbach, *Adv. Mater.* **2011**, *23*, 5641; b) S.-H. Chung, A. Manthiram, *Electrochim. Acta* **2013**, *38*, 568; c) S.-H. Chung, A. Manthiram, *J. Mater. Chem. A* **2013**, *1*, 9590; d) Y.-S. Su, A. Manthiram, *Nat. Commun.* **2012**, *3*, 1166; e) S.-H. Chung, A. Manthiram, *Chem. Commun.* DOI: 10.1039/C4CC00850B; f) K. Zhang, F. Qin, J. Fang, Q. Li, M. Jia, Y. Lai, Z. Zhang, J. Li, *J Solid State Electrochem.* DOI 10.1007/s10008--013--2351--5; g) X. Wang, Z. Wang, L. Chen, *J. Power Sources* **2013**, *242*, 65; h) G. Zhou, S. Pei, L. Li, D.-W. Wang, S. Wang, K. Huang, L.-C. Yin, F. Li, H.-M. Cheng, *Adv. Mater.* **2014**, *26*, 625; i) J. Song, Z. Yu, T. Xu, S. Chen, H. Sohn, M. Regula, D. Wang, *J. Mater. Chem. A* DOI: 10.1039/C4TA00742E.

[7] a) S. Wei, H. Zhang, Y. Huang, W. Wang, Y. Xia, Z. Yu, *Energy Environ. Sci.* **2011**, *4*, 736; b) S.-H. Chung, A. Manthiram, *Adv. Mater.* **2014**, *26*, 1360; c) S.-H. Chung, A. Manthiram, *ChemSusChem* DOI: 10.1002/cssc.201301287.

[8] J. Shim, K. A. Striebel, E. J. Cairns, *J. Electrochem. Soc.* **2002**, *149*, A1321.

[9] S. S. Zhang, J. A. Read, *J. Power Sources* **2012**, *200*, 77.

[10] a) Y.-S. Su, A. Manthiram, *Chem. Commun.* **2012**, *48*, 8817; b) S.-H. Chung, A. Manthiram, *Electrochem. Commun.* **2014**, *38*, 91.

[11] S.-E. Cheon, K.-S. Ko, J.-H. Cho, S.-W. Kim, E.-Y. Chin, H.-T. Kim, *J. Electrochem. Soc.* **2003**, *150*, A800.

[12] a) C. Barchasz, F. Molton, C. Dubo, J.-C. Leprêtre, S. Patoux, F. Alloin, *Anal. Chem.* **2012**, *84*, 3973; b) H. Yamin, A. Gorenshtein, J. Penciner, Y. Sternberg, E. Peled, *J. Electrochem. Soc.* **1988**, *135*, 1045.

[13] S.-E. Cheon, K.-S. Ko, J.-H. Cho, S.-W. Kim, E.-Y. Chin, H.-T. Kim, *J. Electrochem. Soc.* **2003**, *150*, A796.

[14] S. S. Zhang, *Electrochim. Acta* **2013**, *70*, 344.

[15] a) R. D. Rauh, K. M. Abraham, G. F. Pearson, J. K. Surprenant, S. B. Brummer, *J. Electrochem. Soc.* **1979**, *126*, 523; b) F. B. Tudron, J. R. Akridge, V. J. Puglisi, *Proc. 41st Power Sources Conference* Adam's Mark Hotel in Philadelphia (June, **2004**); c) H. S. Ryu, H. J. Ahn, K. W. Kim, J. H. Ahn, J. Y. Lee, E. J. Cairns, *Journal of Power Sources* **2005**, *140*, 365; d) H. S. Ryu, H. J. Ahn, K. W. Kim, J. H. Ahn, K. K. Cho, T. H. Nam, *Electrochim. Acta* **2006**, *52*, 1563.